OXFORD

SOT | Society of Toxicology
www.toxsci.oxfordjournals.org

TOXICOLOGICAL SCIENCES, 153(2), 2016, 372–381

doi: 10.1093/toxsci/kfw133
Advance Access Publication Date: July 29, 2016
Research Article

Alterations in Optineurin Expression and Localization in Pre-clinical Parkinson's Disease Models

John Pierce Wise Jr.* and Jason Cannon*,[1]

*School of Health Sciences, Purdue University, West Lafayette, Indiana 47907

[1]To whom correspondence should be addressed at Associate Professor of Toxicology, Purdue University, 550 Stadium Mall Dr., West Lafayette, IN 47907. Fax: (765) 496-1377, E-mail: cannonjr@purdue.edu.

ABSTRACT

Parkinson's disease (PD) is a progressive neurodegenerative disease that affects ~5 million people around the world. PD etiopathogenesis is poorly understood and curative or disease modifying treatments are not available. Mechanistic studies have identified numerous pathogenic pathways that overlap with many other neurodegenerative diseases. Mutations in the protein optineurin (OPTN) have recently been identified as causative factors for glaucoma and amyotrophic lateral sclerosis. OPTN has multiple recognized roles in neurons, notably in mediating autophagic flux, which has been found to be disrupted in most neurodegenerative diseases. $OPTN^{+}$ aggregates have preliminarily been identified in cytoplasmic inclusions in numerous neurodegenerative diseases, however, whether OPTN has a role in PD pathogenesis has yet to be tested. Thus, we chose to test the hypothesis that OPTN expression and localization would be modulated in pre-clinical PD models. To test our hypothesis, we characterized midbrain OPTN expression in normal rats and in a rat rotenone PD model. For the first time, we show that OPTN is enriched in dopamine neurons in the midbrain, and its expression is modulated by rotenone treatment *in vivo*. Here, animals were sampled at time-points both prior to overt neurodegeneration and after severe behavioral deficits, where a lesion to the nigrostriatal dopamine system is present. The effect and magnitude of OPTN expression changes are dependent on duration of treatment. Furthermore, OPTN colocalizes with LC3 (autophagic vesicle marker) and alpha-synuclein positive puncta in rotenone-treated animals, potentially indicating an important role in autophagy and PD pathogenesis.

Key words: Optineurin; Parkinson's disease; autophagy; rotenone.

Parkinson's disease (PD) pathology is characterized by the progressive loss of dopaminergic (DA) neurons in the substantia nigra (SN) and the formation of Lewy bodies in these and other neurons (Braak *et al.*, 2003; Fornai *et al.*, 2003; Forno, 1996; Gai *et al.*, 2000; Spillantini *et al.*, 1997). Lewy bodies are intracellular inclusions largely composed of aggregated proteins, notably α-synuclein. Despite significant advancements in understanding the genes, proteins, and mechanisms involved, the etiology of PD remains largely unknown. Of note, most data from animal studies is obtained from end-stage models, where significant cell loss and pathology has already occurred. Given that PD is not diagnosed until significant dopaminergic cell loss occurs, there is a critical need to discover molecular pathways affected in the earliest stages of disease (Bernheimer *et al.*, 1973; Fearnley and Lees, 1991).

Whereas the role of Lewy bodies in pathogenesis remains unclear, it is evident that α-synuclein positive inclusions form prior to neuronal loss, suggesting that aberrant protein degradation is a critical early event (Braak *et al.*, 2003). Protein aggregates form by an accumulation of misfolded or damaged proteins that would normally be degraded by autophagy, but autophagy is clearly impaired in PD (Anglade *et al.*, 1997; Higashi *et al.*, 2011; Zhu *et al.*, 2003). This pathway is also responsible for clearing damaged or dysfunctional mitochondria, which are also prevalent in PD (Zhu *et al.*, 2003). Both dysfunctional mitochondria and protein aggregates induce oxidative stress, which may be detrimental to autophagy in conditions of chronic oxidative stress (Dagda *et al.*, 2013). Given that DA neurons of the substantia nigra are characterized by a high basal rate of oxidative stress (Pacelli *et al.*, 2015), it is very likely that impaired

autophagy in these neurons is a critical factor in selective sensitivity to genetic and neurotoxic insults.

Numerous pathways and pathologies overlap in major neurodegenerative diseases (Cannon and Greenamyre, 2011). Thus, there has been significant effort to identify common pathways that lead to risk for neurological diseases. Optineurin (OPTN) is a 577 amino acid protein that is a known genetic link to amyotrophic lateral sclerosis (ALS) and primary open angle and normal tension glaucoma (Maruyama *et al.*, 2010; Sarfarazi and Rezaie, 2003; Ying and Yue, 2012). Of note is that PD patients have a higher risk for the development of glaucoma (Nucci *et al.*, 2015). The OPTN protein contains several putative domains, including a LC3 interacting domain, bZIP motif, 2 leucine zippers, multiple coiled-coil motifs, ubiquitin binding domain, and a C-terminal C_2H_2 type of zinc finger, with numerous binding partners that include LC3, Rab8, Huntingtin, myosin VI, TANK binding kinase 1 (TBK1), ring finger protein 11, serine/threonine kinase receptor interacting protein 1 (RIP1), etc., indicating diverse cellular functions (Chibalina *et al.*, 2008; Swarup and Nagabhushana, 2010; Ying and Yue, 2012). Given the repeatedly identified alterations to autophagy in PD, OPTN's role in this process is of particular interest. To date, the presence of OPTN has been reported to occur in protein inclusions of many neurodegenerative diseases, including ALS, Alzheimer's disease, Huntington's disease, Creutzfeld-Jakob disease, multiple system atrophy, Pick disease, and frontotemporal lobar degeneration (Fujita *et al.*, 2011; Hortobagyi *et al.*, 2011; Mori *et al.*, 2012; Osawa *et al.*, 2011; Schwab *et al.*, 2012). OPTN is also reported to occur in Lewy bodies in PD, although there are major limitations (Osawa *et al.*, 2011). In that study, no control tissue was examined, a single high magnification image of a single cell was shown, and no counterstain was utilized to confirm cell type or that immunoreactivity was due to protein aggregation.

In the present study, we wished to test the hypothesis that based upon known cellular roles, OPTN expression and modulation would be altered in early-stage PD models. For this study we utilized the rat rotenone model, which has been extensively utilized to study PD (Betarbet *et al.*, 2000; Cannon *et al.*, 2009). Rotenone exposure has also been identified as a risk factor for PD (Tanner *et al.*, 2011). Here, for the first time, we have examined OPTN expression in the mammalian midbrain and in preclinical PD models. These studies are expected to be a critical first step to understanding how OPTN may mediate neurodegeneration in PD.

METHODS AND MATERIALS

Animals. All animals were male wild-type Lewis rats purchased from Harlan (now Envigo; Indianapolis, IN) and were between the ages of 31–42 weeks when euthanized. Rats were housed under standard 12 h light cycle, fed ad libitum. All studies were approved by the Purdue University Animal Care and Use Committee.

Chemicals and reagents. Primary antibodies included: rabbit anti-OPTN (ab23666; Abcam, Cambridge, Massachusetts); rabbit anti-OPTN (100000; Cayman Chemical, Ann Arbor, Michigan); mouse anti-LC3 (M152-3; MBL International Corporation, Woburn, Massachusetts); sheep and mouse anti-tyrosine hydroxylase (AB1542, MAB318) were purchased from EMD Millipore (Billerica, Massachusetts); and mouse anti-alpha-synuclein (610786; BD Biosciences, San Jose, California). Secondary antibodies Biotin-SP anti-rabbit (711-065-152), Alexa Fluor 647 anti-sheep (713-605-147), Alexa Fluor 488 anti-rabbit (711-545-152), Cy3 anti-mouse (715-165-151) were purchased from Jackson ImmunoResearch Laboratories, Inc (West Grove, Pennsylvania); IR 800CW anti-mouse (926-32212) was purchased from Licor (Lincoln, Nebraska). Vectastain Elite ABC kit (PK-1600) and DAB Peroxidase (HRP) Substrate kit (SK-4100) were purchased from Vector Laboratories (Burlingame, California). Rotenone (R8875) and glycerol (G5516) were purchased from Sigma-Aldrich (St. Louis, Missouri). DPX mountant was purchased from VWR (100503834, Chicago, Illinois). Triton X-100 was purchased from Fisher BioReagents (BP151-500, Fair Lawn, New Jersey). Histomount was purchased from National Diagnostics (HS-103, Atlanta, Georgia).

Rotenone administration. Rotenone was administered at 3 mg/kg/day by intraperitoneal injection as previously described (Cannon *et al.*, 2009). This model has been extensively characterized in terms of the temporal development of behavioral, neurochemical, and neuropathological alterations in the nigrostriatal dopamine system that are relevant to PD (Cannon and Greenamyre, 2010; Cannon *et al.*, 2009, 2013; Tapias *et al.*, 2010, 2014; Zharikov *et al.*, 2015). Of note, the dose and/or time of exposure can be adjusted to produce a pre-clinical model, where early stage pathogenesis can be studied, prior to overt cell death (Drolet *et al.*, 2009; Sanders *et al.*, 2014a, b). In the present study, we chose to sample animals at both pre-clinical time-points, where overt motor phenotypes were not yet present and at end-stage, where postural instability, rigidity, and bradykinesia were present. These deficits have been well described in the rotenone model at this dose (Cannon *et al.*, 2009). Thus, animals were euthanized after 24 h ($n = 2$), 5 days ($n = 6$), or at end-stage ($n = 8$) (typically at 6-9 days). In this model, overt behavioral deficits are associated with a lesion to the nigrostriatal dopamine system (Betarbet *et al.*, 2000; Cannon *et al.*, 2009), whereas sampling at 5 days or before is prior to the development of a detectable lesion (Sanders *et al.*, 2014a,b).

Immunohistochemistry and silver staining. Rats were put under deep anesthesia with pentobarbital (>50 mg/kg) (Beuthanasia-D Special, Schering-Plough Animal Health Corp, Union, New Jersey), then transcardially perfused with 100–150 ml PBS followed by 250–300 ml 4% buffered paraformaldehyde (PFA). Brains were surgically removed, post-fixed in 4% PFA for approximately 24 h, and then saturated with 30% sucrose at 4 °C for at least 5–7 days until sinking. Each brain was coronally sectioned on a frozen sliding microtome (Microm HM 450, Thermo Scientific) at a 35 μm thickness and stored in cryoprotectant at −20 °C until used for staining. Midbrain sections containing the substantia nigra pars compacta were randomly selected, rinsed in PBS for 10 min, 6 times, at room temperature (RT) on an open air platform shaker.

For colorimetric staining, sections were then quenched in 3% hydrogen peroxide (diluted from 30% hydrogen peroxide, cat. # 5240-05; Macron Fine Chemicals, Center Valley, Pennsylvania); rinsed in PBS again 3 times at RT, 10 min each time (rinsed); blocked in 10% normal donkey serum (NDS, cat. # 017-000-121) in PBS with 0.3% Triton X-100 (PBS-T) for 90 min at RT; incubated with primary antibodies for ~48 h in PBS-T with 1% NDS at 4 °C. Primary antibody concentrations were as follows: rabbit anti-optineurin [Abcam (1:5000) or Cayman (1:100)]. Optimal primary antibody concentrations were determined in pilot studies using graded antibody concentrations. The sections were then rinsed 3 times with PBS at RT for 10 min each time; incubated with secondary antibodies Biotin-SP anti-rabbit (1:200) in PBS-T with 1% NDS for 90 min at RT; rinsed 3 times

with PBS at RT for 10 min each time; incubated in ABC reaction mixture for 60 min at RT; rinsed 3 times with PBS at RT for 10 min each time; incubated in DAB stain until color was visually quenched (typically ~30 s); and rinsed 6 times with PBS at RT for 10 min each time before mounting on slides. DAB-stained sections were mounted on slides and allowed to dry overnight, then dehydrated in graded alcohols and histoclear, and coverslipped using histomount.

For striatal DA terminal density staining; sections were initially rinsed 6 times with PBS at RT for 10 min each time; blocked in 10% normal donkey serum in PBS-T for 90 min at RT; incubated with mouse anti-tyrosine hydroxylase (1:2000) for ~48 h in PBS-T with 1% NDS in PBS-T; rinsed 3 times with PBS at RT for 10 min each time; incubated with IR800 anti-mouse (1:20 000) with 1% NDS in PBS-T for 90 min at RT; and rinsed 6 times with PBS at RT for 10 min each time before mounting on slides. Mounted sections were allowed to dry overnight, then dehydrated in graded alcohols and histoclear, and coverslipped with DPX mountant.

Silver staining was conducted to identify degenerating neurons (Switzer and Butt, 2011). Staining was conducted using FD NeuroSilver Kit II (PK301A; FD NeuroTechnologies, Inc, Columbia, Maryland) from coronal brain sections obtained as described above. Brain tissue was processed according to manufacturer instructions.

For immunofluorescence staining to be analyzed by confocal microscopy, sections were initially rinsed 6 times with PBS at RT for 10 min each time; blocked in 10% NDS in PBS-T for 90 min at RT; incubated with primary antibodies for ~48 h in PBS-T with 1% NDS at 4 °C; rinsed 3 times with PBS at RT for 10 min each time; incubated with secondary antibodies in PBS-T with 1% NDS for 90 min at RT; and rinsed 6 times with PBS at RT for 10 min each time before mounting on slides and coverslipped as a wet mount using 50/50 glycerol:PBS solution. Primary antibody dilutions were: mouse anti-LC3 (1:1000); rabbit anti-optineurin (1:5000); sheep anti-tyrosine hydroxylase (1:1000); mouse anti-alpha synuclein (1:2000). Secondary antibody dilutions were: Alexa Fluor 647 anti-sheep, Alexa Fluor 488 anti-rabbit, or Cy3 anti-mouse (1:500).

Microscopy and image analysis. Light microscopy images were captured on an Olympus System Microscope Model BX53 with an Olympus digital camera model DP72 (12.8 megapixel, color), and using the Olympus cellSens Dimensions software (ver. 1.14).

To verify the expected temporal development of the rotenone-induced lesion to the nigrostriatal dopamine system, we qualitatively analyzed DA striatal terminal density by fluorescently detecting tyrosine hydroxylase (TH) as previously described (Cannon *et al.*, 2011; Lee *et al.*, 2015; Tapias *et al.*, 2014). For this experiment, 1 in 12 striatal sections from each animal were stained using mouse anti-TH primary antibody and IR 800CW anti-mouse secondary antibody. Immunolabeled sections were scanned at 800 nm on an Odyssey Infrared Imaging System (Licor Inc., Lincoln, Nebraska) at a resolution of 42 μm.

Confocal images were captured on an inverted Nikon fully motorized Ti-E microscope equipped with ×10, ×20 and ×60 high NA oil immersion objectives. Region of interest analysis was then conducted on images using the NIS-Elements software ver. 4.30 to measure signal intensity. High magnification images (×60) were analyzed for puncta analysis; puncta were considered bright circular dots with diameters ranging from 0.5 to 1.5 μm, as has been previously described for autophagosome diameters (Klionsky *et al.*, 2016).

Statistical analysis. Statistical analysis was conducted using GraphPad PRISM, ver. 6. Data for intensity and puncta analyses were found not to have a Gaussian distribution by the D'Agostino & Pearson omnibus normality test. Thus, nonparametric analysis was conducted using Kruskal–Wallis nonparametric ANOVA, followed by *post-hoc* analysis using the Dunn's test. $P < .05$ deemed significant for all tests.

RESULTS

OPTN in the Rat Midbrain and Striatum

Immunostaining with colorimetric development in untreated rats clearly shows that in the midbrain, OPTN is enriched in the pars compacta region of the substantia nigra (primary antibody from Abcam as noted in Methods) (Figs. 1A–C). In the midbrain specifically, expression appears to be far higher in the substantia nigra than in surrounding nuclei. Expression also appears to be high in pyramidal neurons of the hippocampus and in cortical layers 1 and 2. Colocalization of OPTN with TH by immunofluorescence using confocal microscopy clearly shows high expression in DA neurons, with limited expression in non-dopaminergic neurons (Figs. 1D–F). Expression is also evident in the medial DAergic ventral tegmental area. Additional stainings conducted with a second primary antibody generated from a different epitope and supplier revealed a similar staining pattern (supplied by Cayman Chemical as noted in the "Materials and Methods" section) (data not shown).

OPTN staining in the striatum showed an overall diffuse expression (Figure 2A). Axon terminals within the striatum do not overtly express OPTN (Figure 2B), although some interneurons exhibit expression. Cellular expression was also noted in the cortex (Figure 2C) and lateral septum (Figure 2D), though enrichment was not nearly as striking as in dopaminergic neurons in the substantia nigra (Figure 1).

Temporal Development of a Lesion to the Nigrostriatal Dopamine System

We confirmed that our 24 h and 5-day sampling points did not exhibit an overt lesion to the nigrostriatal DA system, as expected based on the literature and our extensive experience with this model. Low magnification immunofluorescent images of coronal sections from the striatum that were stained for TH show no overt lesion in controls or animals treated with rotenone for 24 h or 5 days. However, an overt lesion of DA terminals is clearly evident in animals treated until the emergence of severe behavioral deficits (Figure 3). Further, silver staining shows that argyrophilic cells are notable after 5 days of rotenone treatment (Figs. 3E–H) and upon the emergence of end-stage behavioral deficits, there is an apparent loss of large, angular cells, with a morphology characteristic of DA neurons. These findings are highly consistent with numerous published detailed pathological and mechanistic reports in this model, where lesion development has been extensively quantified (Cannon *et al.*, 2009; Sanders *et al.*, 2014a, b; Tapias *et al.*, 2010, 2014).

Rotenone Alters OPTN Expression in Relation to Autophagic Activity and alpha-Synuclein Puncta

Given OPTN's known roles in autophagy in neurodegenerative diseases (eg, glaucoma, ALS, Huntington's disease) and autophagy's roles in PD, we examined a potential role for OPTN in PD-relevant autophagic dysfunction. Initially, we examined whether overt changes in OPTN expression were temporally

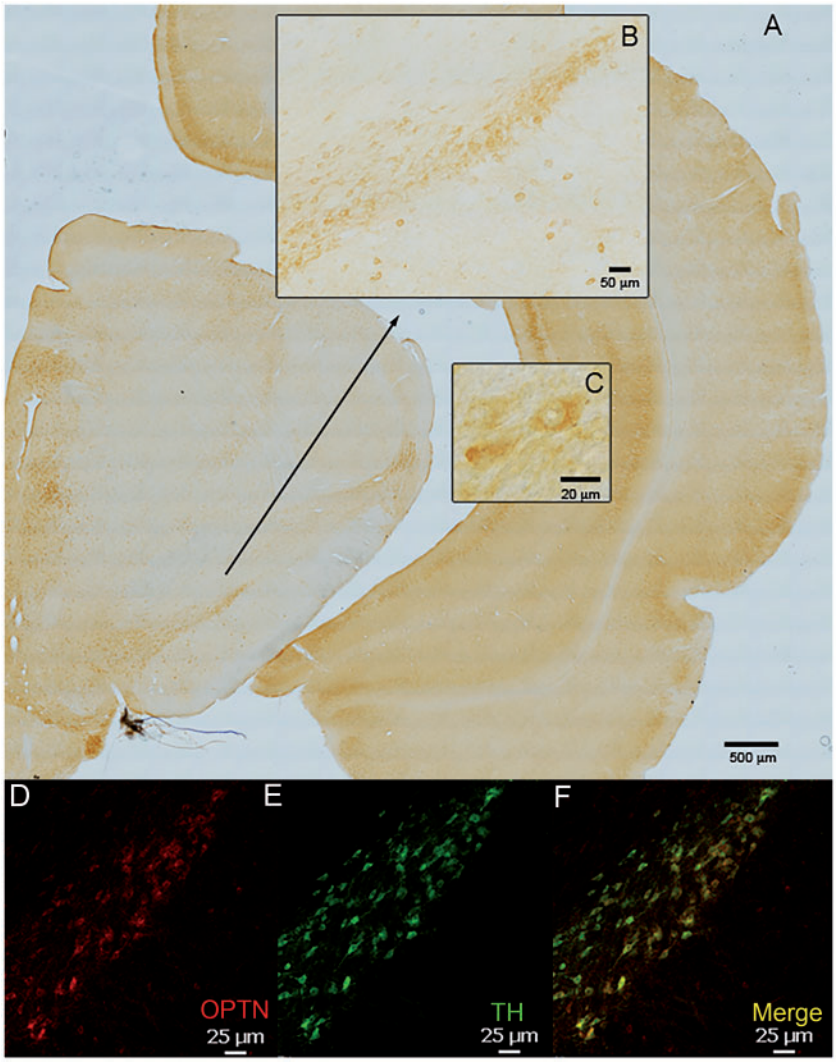

FIG. 1. OPTN expression is enriched in dopaminergic neurons of the substantia nigra. (A–C) Untreated rat coronal midbrain section stained for OPTN at × 10, ×20, and ×40, respectively (scale bars = 500, 50, 20 μm, respectively). (D-F) Double immunofluorescent stained section with colocalization of tyrosine hydroxylase (TH) (DA neurons) and OPTN within the substantia nigra validate OPTN expression is in DA neurons; OPTN in red, TH in green, colocalized in yellow. Scale bar = 25 μm.

related to nigrostriatal DA lesion development. Figure 4 shows DAB-immunostained OPTN in each stage. Colorimetric staining indicated that OPTN expression increased with rotenone exposure and that localization appeared to shift into puncta. This finding suggested that quantitative analyses of both whole cell OPTN expression (conducted in Figure 5E) and puncta localization (conducted in Figs. 5 G–I) was warranted.

We investigated the possibility that OPTN puncta may relate to rotenone-induced changes in autophagy by co-staining nigral tissues of our staged rats with TH, OPTN, and LC3 (autophagy biomarker). Our results clearly show OPTN and LC3 colocalization in puncta 0.5–1.5 μm in diameter (Figs. 5A–D), the typical size range of autophagosomes. We considered changes in expression of each protein by measuring the relative intensity within the cell soma; our analysis indicates an increase in OPTN expression in rotenone groups [100 ± 2.27 vs 136.64 ± 5.89, 121.10 ± 1.97, 141.59 ± 4.25; mean (normalized to control) ± SEM for control, 24 h, 5 day, respectively; $P < .05$ from control, Dunn's multiple comparison test after significant Kruskal–Wallis test; $n = 131$–358 cells analyzed/group from 2 to 5 animals] (Figs. 5A–E). We found that total LC3 expression increases after only a single rotenone dose; we observed an initial increase in LC3 expression after 24 h rotenone with a temporal decrease near control levels at 5 days and end-stage expression in rotenone groups (100 ± 1.23 vs 125.77 ± 3.60, 92.73 ± 0.71, 96.41 ± 1.38 mean (normalized to control) ± SEM for control, for control, 24 h, 5 days, end-stage, respectively; $P < .05$ from control, Dunn's multiple comparison test after significant Kruskal–Wallis test) (Figs. 5A–D, F). Further, OPTN was found to be associated with changes in autophagic vesicle number through puncta analysis. Puncta number per cell for $OPTN^+$; $LC3^+$; $OPTN^+/LC3^+$ puncta were quantified (Figs. 5G–I). We observed an increase in the average number of OPTN puncta per cell that became statistically significant in 5 days or end-stage groups (16.70 ± 0.66 vs 19.55 ± 0.59, 19.71 ± 0.49 mean ± SEM for control, for control, 5 days, end-stage, respectively; $P < .05$ from control, Dunn's multiple comparison test after significant Kruskal–Wallis test). LC3 puncta showed a biphasic response relative to rotenone treatment, with an increase that was only detectable at 5 days (11.89 ± 0.49 vs 14.33 ± 0.45 mean ± SEM for control, for control and 5 days, respectively; $P < .05$ from control, Dunn's multiple comparison test after significant Kruskal–Wallis

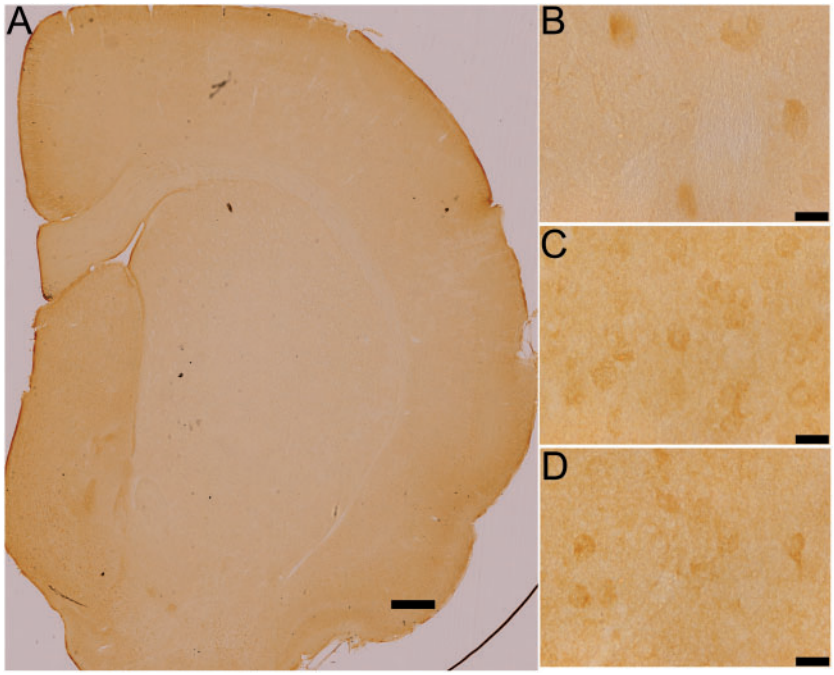

FIG. 2. OPTN expression in the striatum. (A) Low magnification coronal section of striatum stained for OPTN (bar = 500 μm). (**B-C**) High magnification images of dorsolateral striatum **(B),** cortex (C), and lateral septum (D). Scale bar = 25 μm.

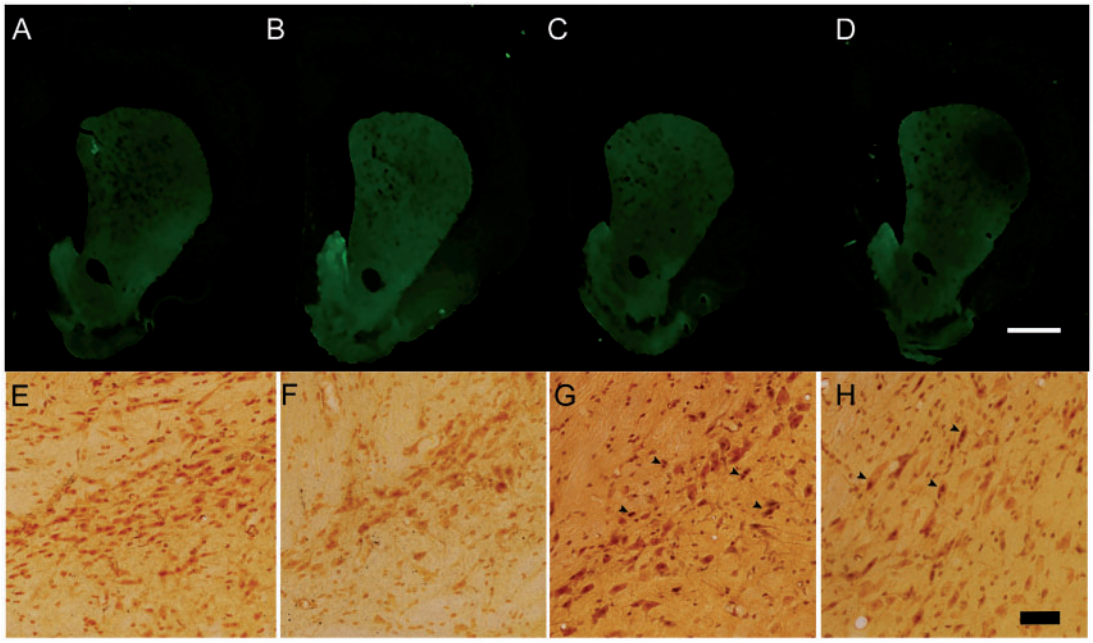

FIG. 3. An overt lesion to the nigrostriatal dopamine system does not occur until the emergence of behavioral deficits. (A–D) Representative images of striatal TH terminal densities indicate significant striatal lesion in end-stage models and with no visual lesion in pre-clinical models; (A) control treated with DMSO, (B) 24 h rotenone, (C) 5-day rotenone, and (D) treatment until end-stage behavioral phenotype presented. Scale bar = 500 μm. (E-H) Silver staining in the pars compacta region of the substantia nigra showing limited affinity in (E) control and (F) 24 h rotenone. Cells become argyrophilic (arrowheads show examples) after (G) 5-day rotenone, and (H) upon treatment until end-stage behavioral phenotype emerges, there is an expected decrease of large, angular neurons consistent with dopaminergic neuron morphology. Scale bar = 50 μm.

test). A similar phenomenon was observed for puncta expressing both LC3 and OPTN, where increases were detectable only at 5 days (8.27 ± 0.35 vs 10.81 ± 0.40 mean ± SEM for control, for control and 5 days, respectively; $P < .05$ from control, Dunn's multiple comparison test after significant Kruskal–Wallis test).

Alpha-synuclein staining, along with TH and OPTN shows increasing OPTN puncta similar to Figure 5 that largely colocalize with alpha-synuclein positive puncta (Figure 6). Alpha-synuclein positive puncta appear to increasingly colocalize with OPTN as the number of rotenone treatments increase. Representative images were shown from >50 images collected per group.

Thus, in pre-clinical and end-stage neurotoxicant-induced PD models, changes in OPTN expression, localization and

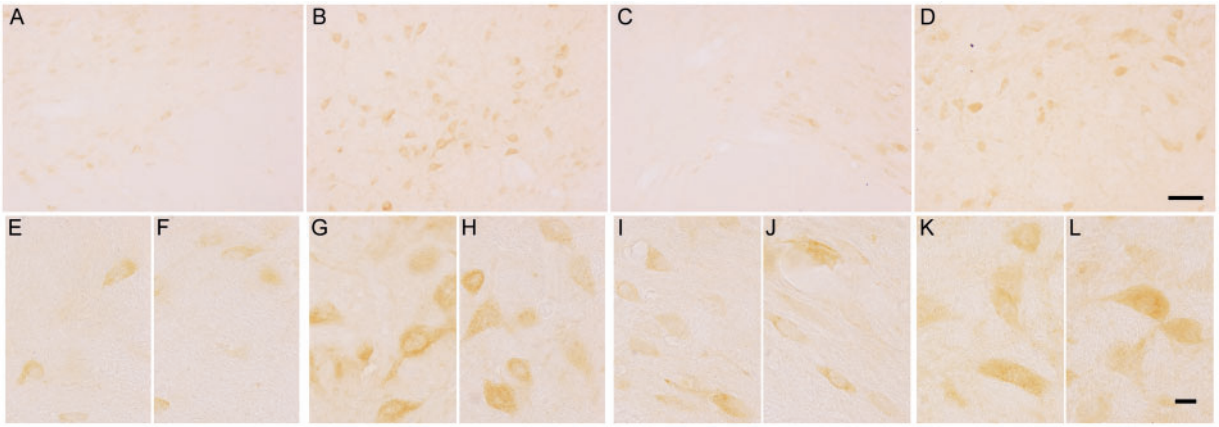

FIG. 4. OPTN expression in the substantia nigra increases in pre-clinical and end-stage PD models. Representative images of nigral dopamine neurons stained for OPTN in Lewis rats treated with DMSO (control; A, E, F) or 3.0 mg/kg/day rotenone i.p. for 24 h (B, G, H), 5 days (C, I, J), or until end-stage behavioral phenotype (D, K, L) to model different stages of PD, respectively. (A–D) Low magnification (×20) representative images of OPTN-positive cells in the substantia nigra pars compacta of rats from each stage. (E–L) High magnification (×60) representative images of OPTN-positive cells in the substantia nigra pars compacta region of rats from each stage. Scale bar = 50 μm (A–D), 10 μm (E–L).

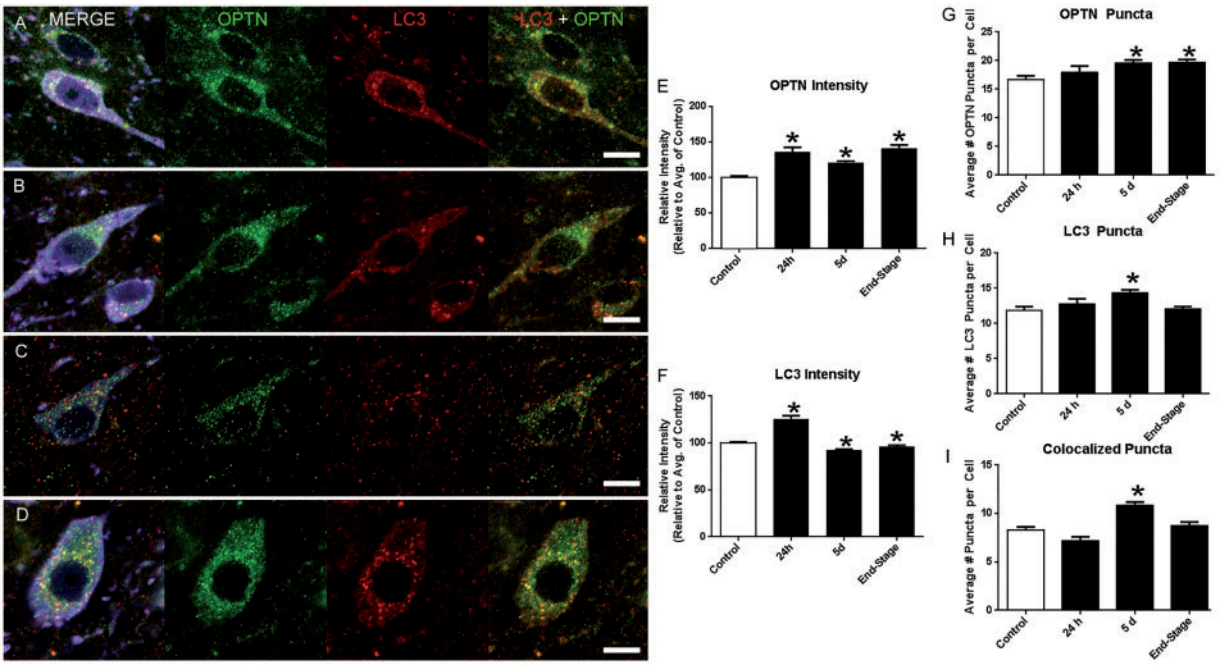

FIG. 5. OPTN expression, aggregation, and colocalization with LC3 increases in pre-clinical and end-stage PD models. (A–D) Representative images of nigral dopamine cells co-stained with OPTN, LC3 and TH from animals treated as control, 24 h, 5 days, and end stage, respectively; TH in blue, OPTN in green, LC3 in red, colocalized OPTN/LC3 in yellow. Scale bar = 10 μm. (E–F) Quantitative analysis of OPTN and LC3 expression, respectively, measured by relative intensity of total cellular expression (relative to control); (G–I) mean number of puncta per cell for OPTN, LC3, or colocalized puncta, respectively, across stages; data are presented as mean ± SEM; *$P < .05$ from control, Dunn's multiple comparison test after significant Kruskal–Wallis test.

relation to autophagosomes and alpha-synuclein positive puncta clearly occur, and in many cases prior to lesion formation. These changes occur within DA neurons (TH^+).

DISCUSSION

There is considerable overlap in many pathological processes between neurodegenerative diseases. Given known roles in cellular processes that are disrupted in neurodegenerative diseases, the protein OPTN is a plausible important effector. Whereas OPTN mutations have been linked to several neurodegenerative diseases, the protein has received minimal attention in PD research. For the first time, we show that OPTN expression is enriched in DA neurons in the midbrain, and that expression is modulated in a neurotoxic PD model. Notably, changes occur prior to an overt lesion. It is expected that these findings will prompt follow-up mechanistic investigations to determine if OPTN is a critical mediator of PD pathogenesis.

OPTN has numerous structural motifs linked to many roles in the cell including: vesicle trafficking, Golgi structural protein, an autophagic cargo adaptor, transcription factor, and in the innate immune system (Ying and Yue, 2012). OPTN point mutations have been linked to glaucoma or ALS and evidence

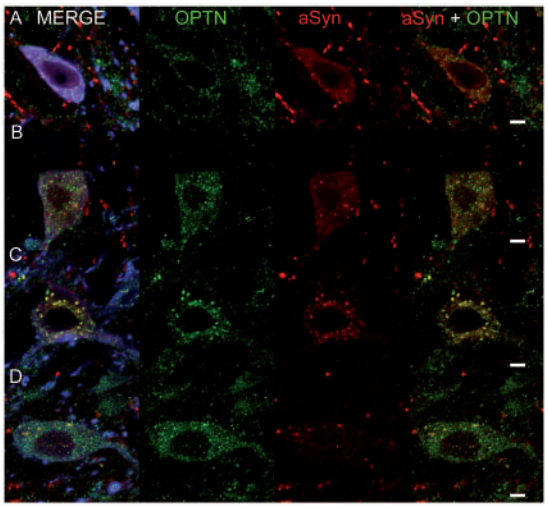

FIG. 6. OPTN and alpha-synuclein expression in pre-clinical and end-stage PD models. OPTN and alpha-synuclein positive puncta increase with rotenone treatment. (A–D) Representative images of nigral dopamine cells co-stained with OPTN, alpha-synuclein and TH from animals treated as control, 24 h, 5 days, and end stage, respectively; TH in blue, OPTN in green, alpha-synuclein in red, colocalized OPTN/alpha-synuclein in yellow. Scale bar = 5 μm.

implicates impaired autophagy and compromised mitochondrial integrity as key pathogenic mechanisms (Chalasani *et al.*, 2014; Sirohi *et al.*, 2015; Wong and Holzbaur, 2014). Autophagy disruptions and mitochondrial dysfunction occur in PD and are likely key pathogenic events in the earliest disease stages (Parker *et al.*, 1989; Tan *et al.*, 2014). PD patients also have a higher risk for glaucoma (Nucci *et al.*, 2015). Further, meta-analysis of genome-wide association studies shows that single nucleotide polymorphisms in OPTN may increase PD risk. Specifically, the M98K mutation, which likely affects OPTN-mediated autophagy, causes glaucoma and was identified as a PD risk modulator (Lill *et al.*, 2012; Sirohi *et al.*, 2015). Thus, mechanistic and genetic data provide a strong rationale for investigation in PD.

To date, there is a single human report on OPTN in PD and no known animal model studies. The human study focused on comparing intracellular OPTN aggregates across several neurodegenerative diseases (Osawa *et al.*, 2011). With respect to PD, there are many limitations in this initial report: (1) no control tissue was stained; (2) a single cell was shown in a high-magnification image; (3) a single possible Lewy neurite was shown, though this image possibly shows a blood vessel; (4) no counterstain was used to confirm that expression was in a neuron. Given known OPTN functions, and relevance to PD, we chose to conduct the first study of OPTN expression in normal animals and in PD models.

In the midbrain, we found OPTN expression to be enriched in the substantia nigra, particularly in the pars compacta region (Figure 1). Expression also appears to be high in pyramidal neurons of the hippocampus and in cortical layers 1 and 2. Whereas expression is not exclusive to the nigra, staining intensity is clearly higher than in surrounding regions. Through immunofluorescence staining and confocal microscopy, we confirmed expression in DA neurons, which appears to be higher than in non-DA neurons. Expression appears to be primarily limited to the soma, as there was not clear evidence of terminal staining in the striatum (Figure 2). Proteins enriched in nigral DA neurons typically have important roles in DA cell survival (Bissonette and Roesch, 2016). Thus, our findings suggest that mechanistic studies to determine how OPTN influences dopamine neuron integrity should be conducted. Further, whole brain, cell-type specific expression analysis should be conducted in the future to characterize expression in other major brain nuclei, particularly those affected in PD.

For toxicant response studies, we utilized the rat rotenone model. Rotenone exposure is a PD risk factor in humans and rotenone has been used extensively to model the disease in animals (Cannon and Greenamyre, 2010; Tanner *et al.*, 2011). Here, rotenone exposure was utilized to produce models of different stages of PD by dosing the rats with 3 mg/kg/day rotenone for 24 h (to model very early stage), 5 days (to model early-mid stage), and until animals exhibited severe motor deficits (typically beginning at ~7 days) (Cannon *et al.*, 2009). The emergence of qualitative behavioral deficits such as bradykinesia, postural insatiability, and rigidity have been shown to coincide with development of a lesion to the nigrostriatal dopamine system characteristic of late stage PD (Cannon *et al.*, 2009). This specific model has been extensively characterized in terms of the temporal development of quantitative behavioral deficits and the emergence of a lesion to the nigrostriatal DA system (Cannon *et al.*, 2009, 2013; Tapias *et al.*, 2010, 2014; Zharikov *et al.*, 2015). Of note, sampling time can easily be adjusted to obtain a "pre-clinical" model, where endpoints are assessed prior to the emergence of a behavioral phenotype and overt lesion to the nigrostriatal DA system (Cannon and Greenamyre, 2014; Sanders *et al.*, 2014a, 2014b). Thus, this model offered unique advantages with respect to environmental relevance, replication of key pathologies, and availability of sampling time-points akin to pre-clinical time-points in humans. Our findings confirmed expected lesion development with respect to striatal TH terminal density and nigral silver staining—only the end stage animals exhibited an obvious striatal lesion and overt neuronal loss (Figure 3). These findings are highly consistent with our many publications in this model and confirm suitability of early time-points for pre-clinical assessment (Cannon and Greenamyre, 2014). Examination of changes in OPTN expression and localization in other environmental and genetic animal models will strengthen conclusions on a potential role in PD.

In rotenone treated animals, immunohistological staining with chromogenic development (DAB) for OPTN showed possible increases in expression and increased localization in puncta. Specifically, subcellular staining appeared to be more punctate in later PD stage models than in controls (Figure 4). Thus, we chose to conduct quantitative immunofluorescence studies to further identify changes in whole cell expression (Figure 5E) and localization (Figure 5G). Given known roles in autophagy, we suspected that OPTN may localize to autophagosomes. To investigate the OPTN puncta, we conducted fluorescent immunohistochemistry, using antibodies against OPTN and LC3 with TH as a cellular marker of dopaminergic neurons. Here, we found a significant proportion of the OPTN puncta to be colocalized with LC3 (biomarker for macroautophagy) in punctate structures within the known size range for macroautophagy (Figures 5A–D, I) (Klionsky *et al.*, 2016). Furthermore, OPTN and LC3 puncta followed a similar pattern of incidence across PD stage models; puncta increased with later PD stages. Our results show a decrease in LC3 and colocalized puncta from 5-day to end-stage models, but OPTN puncta number remains the same. Further experiments will need to be conducted to determine why this discrepancy occurred, but we can surmise some possible explanations. Possible explanations are that fewer autophagosomes were created in the cells of end-stage animals, which

led to fewer colocalized puncta, independent of OPTN mediated autophagy or that severe autophagic stress resulted in cell death. A more detailed examination of the data shows approximately 16% decrease in LC3 puncta and approximately 20% decrease in colocalized puncta—this discrepancy could be in part due to changes in phosphorylation of OPTN. Previous studies have demonstrated phosphorylation of human OPTN on Ser177 (likely Ser188 in rat) is critical for its role in autophagy, blocking this phosphorylation site significantly delays autophagic clearance of cargo (Korac *et al.*, 2013; Rogov *et al.*, 2013; Wild *et al.*, 2011).

OPTN expression is known to be regulated by the autophagy regulator transcription factor EB (TFEB) and the inflammatory cytokine TNF-alpha (Nagabhushana *et al.*, 2011; Visvikis *et al.*, 2014). Both autophagic dysfunction and neuroinflammation occur in PD and are linked to pathogenesis (Macchi *et al.*, 2015; Tan *et al.*, 2014). OPTN itself is typically degraded by the proteasome, and is a known autophagy cargo adaptor (Shen *et al.*, 2011). Thus, our data showing LC3 colocalization strongly suggest puncta stem from autophagic vesicles, instead of aberrant OPTN degradation (Shen *et al.*, 2011). Overall, our findings are consistent with the observations that autophagy is impaired in PD brains and models, where alpha-synuclein accumulation has been intensely investigated (Mader *et al.*, 2012; Tan *et al.*, 2014). Alpha-synuclein is a pivotal PD protein linked to the pathogenesis and progression of sporadic and genetic PD (Braak *et al.*, 2004; Polymeropoulos *et al.*, 1997; Spillantini *et al.*, 1997). Alpha-synuclein increases are replicated in the rat rotenone model (Betarbet *et al.*, 2000). Here, we show evidence (Figure 6) that OPTN localization with alpha-synuclein positive intracellular puncta are increasingly evident in rotenone treated animals. Given that alpha-synuclein can be degraded by the ubiquitin-proteasome pathway, chaperone mediated autophagy, and macroautophagy, targeted studies will be required to understand OPTN and alpha-synuclein interactions (Lopes da Fonseca *et al.*, 2015). Mechanistic *in vitro* studies will need to be conducted in the future to confirm and understand the role of OPTN in mediating aberrant autophagy and PD-relevant neurotoxicity.

In summary, we provide the first evidence of OPTN in the rodent midbrain and that expression and localization may be modulated in pre-clinical and end-stage environmentally relevant PD models. Our data suggest that OPTN-associated changes in autophagy may be linked to progression of a nigrostriatal dopamine lesion. Future studies are aimed at a more thorough mechanistic examination and whether OPTN may be a therapeutic target.

ACKNOWLEDGMENTS

Adriaan de Feijter and Kim Freeman for microscope technical support.

FUNDING

National Institute of Environmental Health Sciences at the National Institutes of Health (grant numbers R00ES019879, R03ES022819, R01ES025750 to J.R.C.).

REFERENCES

Anglade, P., Vyas, S., Hirsch, E. C., and Agid, Y. (1997). Apoptosis in dopaminergic neurons of the human substantia nigra during normal aging. *Histol. Histopathol.* **12**, 603–610.

Bernheimer, H., Birkmayer, W., Hornykiewicz, O., Jellinger, K., and Seitelberger, F. (1973). Brain dopamine and the syndromes of Parkinson and Huntington. Clinical, morphological and neurochemical correlations. *J. Neurol. Sci.* **20**, 415–455.

Betarbet, R., Sherer, T. B., MacKenzie, G., Garcia-Osuna, M., Panov, A. V., and Greenamyre, J. T. (2000). Chronic systemic pesticide exposure reproduces features of Parkinson's disease. *Nat. Neurosci.* **3**, 1301–1306.

Bissonette, G. B., and Roesch, M. R. (2016). Development and function of the midbrain dopamine system: What we know and what we need to. *Genes Brain Behav.* **15**, 62–73.

Braak, H., Del Tredici, K., Rub, U., de Vos, R. A., Jansen Steur, E. N., and Braak, E. (2003). Staging of brain pathology related to sporadic Parkinson's disease. *Neurobiol. Aging* **24**, 197–211.

Braak, H., Ghebremedhin, E., Rub, U., Bratzke, H., and Del Tredici, K. (2004). Stages in the development of Parkinson's disease-related pathology. *Cell Tissue Res.* **318**, 121–134.

Cannon, J. R., Geghman, K. D., Tapias, V., Sew, T., Dail, M. K., Li, C., and Greenamyre, J. T. (2013). Expression of human E46K-mutated alpha-synuclein in BAC-transgenic rats replicates early-stage Parkinson's disease features and enhances vulnerability to mitochondrial impairment. *Exp. Neurol.* **240**, 44–56.

Cannon, J. R., and Greenamyre, J. T. (2010). Neurotoxic in vivo models of Parkinson's disease recent advances. *Prog. Brain Res.* **184**, 17–33.

Cannon, J. R., and Greenamyre, J. T. (2011). The role of environmental exposures in neurodegeneration and neurodegenerative diseases. *Toxicol. Sci.* **124**, 225–250.

Cannon, J. R., and Greenamyre, J. T. (2014). Rotenone as preclinical model compound in Parkinson disease. In *Handbook of Neurotoxicity* (R. M. Kostrzewa, Ed.), pp. 995–1012. Springer, New York, NY.

Cannon, J. R., Sew, T., Montero, L., Burton, E. A., and Greenamyre, J. T. (2011). Pseudotype-dependent lentiviral transduction of astrocytes or neurons in the rat substantia nigra. *Exp. Neurol.* **228**, 41–52.

Cannon, J. R., Tapias, V., Na, H. M., Honick, A. S., Drolet, R. E., and Greenamyre, J. T. (2009). A highly reproducible rotenone model of Parkinson's disease. *Neurobiol. Dis.* **34**, 279–290.

Chalasani, M. L., Kumari, A., Radha, V., and Swarup, G. (2014). E50K-OPTN-induced retinal cell death involves the Rab GTPase-activating protein, TBC1D17 mediated block in autophagy. *PLoS One* **9**, e95758.

Chibalina, M. V., Roberts, R. C., Arden, S. D., Kendrick-Jones, J., and Buss, F. (2008). Rab8-optineurin-myosin VI: Analysis of interactions and functions in the secretory pathway. *Methods Enzymol.* **438**, 11–24.

Dagda, R. K., Das Banerjee, T., and Janda, E. (2013). How Parkinsonian toxins dysregulate the autophagy machinery. *Int. J. Mol. Sci.* **14**, 22163–22189.

Drolet, R. E., Cannon, J. R., Montero, L., and Greenamyre, J. T. (2009). Chronic rotenone exposure reproduces Parkinson's disease gastrointestinal neuropathology. *Neurobiol. Dis.* **36**, 96–102.

Fearnley, J. M., and Lees, A. J. (1991). Ageing and Parkinson's disease: Substantia nigra regional selectivity. *Brain* **114**, 2283–2301.

Fornai, F., Lenzi, P., Gesi, M., Ferrucci, M., Lazzeri, G., Natale, G., Ruggieri, S., and Paparelli, A. (2003). Recent knowledge on molecular components of Lewy bodies discloses future therapeutic strategies in Parkinson's disease. *Curr. Drug Targets CNS Neurol. Disord.* **2**, 149–152.

Forno, L. S. (1996). Neuropathology of Parkinson's disease. *J. Neuropathol. Exp. Neurol.* **55**, 259–272.

Fujita, K., Yoshida, M., Sako, W., Maeda, K., Hashizume, Y., Goto, S., Sobue, G., Izumi, Y., and Kaji, R. (2011). Brainstem and spinal cord motor neuron involvement with optineurin inclusions in proximal-dominant hereditary motor and sensory neuropathy. *J. Neurol. Neurosurg. Psychiatry* **82**, 1402–1403.

Gai, W. P., Yuan, H. X., Li, X. Q., Power, J. T., Blumbergs, P. C., and Jensen, P. H. (2000). In situ and in vitro study of colocalization and segregation of alpha-synuclein, ubiquitin, and lipids in Lewy bodies. *Exp. Neurol.* **166**, 324–333.

Higashi, S., Moore, D. J., Minegishi, M., Kasanuki, K., Fujishiro, H., Kabuta, T., Togo, T., Katsuse, O., Uchikado, H., Furukawa, Y., *et al.* (2011). Localization of MAP1-LC3 in vulnerable neurons and Lewy bodies in brains of patients with dementia with Lewy bodies. *J. Neuropathol. Exp. Neurol.* **70**, 264–280.

Hortobagyi, T., Troakes, C., Nishimura, A. L., Vance, C., van Swieten, J. C., Seelaar, H., King, A., Al-Sarraj, S., Rogelj, B., and Shaw, C. E. (2011). Optineurin inclusions occur in a minority of TDP-43 positive ALS and FTLD-TDP cases and are rarely observed in other neurodegenerative disorders. *Acta Neuropathol.* **121**, 519–527.

Klionsky, D. J., Abdelmohsen, K., Abe, A., Abedin, M. J., Abeliovich, H., Acevedo Arozena, A., Adachi, H., Adams, C. M., Adams, P. D., Adeli, K., *et al.* (2016). Guidelines for the use and interpretation of assays for monitoring autophagy, 3rd ed. *Autophagy* **12**, 1–222.

Korac, J., Schaeffer, V., Kovacevic, I., Clement, A. M., Jungblut, B., Behl, C., Terzic, J., and Dikic, I. (2013). Ubiquitin-independent function of optineurin in autophagic clearance of protein aggregates. *J. Cell Sci.* **126**, 580–592.

Lee, J. W., Tapias, V., Di Maio, R., Greenamyre, J. T., and Cannon, J. R. (2015). Behavioral, neurochemical, and pathologic alterations in bacterial artificial chromosome transgenic G2019S leucine-rich repeated kinase 2 rats. *Neurobiol. Aging* **36**, 505–518.

Lill, C. M., Roehr, J. T., McQueen, M. B., Kavvoura, F. K., Bagade, S., Schjeide, B. M., Schjeide, L. M., Meissner, E., Zauft, U., Allen, N. C., *et al.* (2012). Comprehensive research synopsis and systematic meta-analyses in Parkinson's disease genetics: The PDGene database. *PLoS Genet.* **8**, e1002548.

Lopes da Fonseca, T., Villar-Pique, A., and Outeiro, T. F. (2015). The interplay between alpha-synuclein clearance and spreading. *Biomolecules* **5**, 435–471.

Macchi, B., Di Paola, R., Marino-Merlo, F., Felice, M. R., Cuzzocrea, S., and Mastino, A. (2015). Inflammatory and cell death pathways in brain and peripheral blood in Parkinson's disease. *CNS Neurol. Disord. Drug Targets* **14**, 313–324.

Mader, B. J., Pivtoraiko, V. N., Flippo, H. M., Klocke, B. J., Roth, K. A., Mangieri, L. R., and Shacka, J. J. (2012). Rotenone inhibits autophagic flux prior to inducing cell death. *ACS Chem. Neurosci.* **3**, 1063–1072.

Maruyama, H., Morino, H., Ito, H., Izumi, Y., Kato, H., Watanabe, Y., Kinoshita, Y., Kamada, M., Nodera, H., Suzuki, H., *et al.* (2010). Mutations of optineurin in amyotrophic lateral sclerosis. *Nature* **465**, 223–226.

Mori, F., Tanji, K., Toyoshima, Y., Yoshida, M., Kakita, A., Takahashi, H., and Wakabayashi, K. (2012). Optineurin immunoreactivity in neuronal nuclear inclusions of polyglutamine diseases (Huntington's, DRPLA, SCA2, SCA3) and intranuclear inclusion body disease. *Acta Neuropathol.* **123**, 747–749.

Nagabhushana, A., Bansal, M., and Swarup, G. (2011). Optineurin is required for CYLD-dependent inhibition of TNFalpha-induced NF-kappaB activation. *PLoS One* **6**, e17477.

Nucci, C., Martucci, A., Cesareo, M., Garaci, F., Morrone, L. A., Russo, R., Corasaniti, M. T., Bagetta, G., and Mancino, R. (2015). Links among glaucoma, neurodegenerative, and vascular diseases of the central nervous system. *Prog. Brain Res.* **221**, 49–65.

Osawa, T., Mizuno, Y., Fujita, Y., Takatama, M., Nakazato, Y., and Okamoto, K. (2011). Optineurin in neurodegenerative diseases. *Neuropathology* **31**, 569–574.

Pacelli, C., Giguere, N., Bourque, M. J., Levesque, M., Slack, R. S., and Trudeau, L. E. (2015). Elevated mitochondrial bioenergetics and axonal arborization size are key contributors to the vulnerability of dopamine neurons. *Curr. Biol.* **25**, 2349–2360.

Parker, W. D., Jr., Boyson, S. J., and Parks, J. K. (1989). Abnormalities of the electron transport chain in idiopathic Parkinson's disease. *Ann. Neurol.* **26**, 719–723.

Polymeropoulos, M. H., Lavedan, C., Leroy, E., Ide, S. E., Dehejia, A., Dutra, A., Pike, B., Root, H., Rubenstein, J., Boyer, R., *et al.* (1997). Mutation in the alpha-synuclein gene identified in families with Parkinson's disease. *Science* **276**, 2045–2047.

Rogov, V. V., Suzuki, H., Fiskin, E., Wild, P., Kniss, A., Rozenknop, A., Kato, R., Kawasaki, M., McEwan, D. G., Lohr, F., *et al.* (2013). Structural basis for phosphorylation-triggered autophagic clearance of Salmonella. *Biochem. J.* **454**, 459–466.

Sanders, L. H., Howlett, E. H., McCoy, J., and Greenamyre, J. T. (2014a). Mitochondrial DNA damage as a peripheral biomarker for mitochondrial toxin exposure in rats. *Toxicol. Sci.* **142**, 395–402.

Sanders, L. H., McCoy, J., Hu, X., Mastroberardino, P. G., Dickinson, B. C., Chang, C. J., Chu, C. T., Van Houten, B., and Greenamyre, J. T. (2014b). Mitochondrial DNA damage: Molecular marker of vulnerable nigral neurons in Parkinson's disease. *Neurobiol. Dis.* **70**, 214–223.

Sarfarazi, M., and Rezaie, T. (2003). Optineurin in primary open angle glaucoma. *Ophthalmol. Clin. North Am.* **16**, 529–541.

Schwab, C., Yu, S., McGeer, E. G., and McGeer, P. L. (2012). Optineurin in Huntington's disease intranuclear inclusions. *Neurosci. Lett.* **506**, 149–154.

Shen, X., Ying, H., Qiu, Y., Park, J. S., Shyam, R., Chi, Z. L., Iwata, T., and Yue, B. Y. (2011). Processing of optineurin in neuronal cells. *J. Biol. Chem.* **286**, 3618–3629.

Sirohi, K., Kumari, A., Radha, V., and Swarup, G. (2015). A glaucoma-associated variant of optineurin, M98K, activates Tbk1 to enhance autophagosome formation and retinal cell death dependent on Ser177 phosphorylation of optineurin. *PLoS One* **10**, e0138289.

Spillantini, M. G., Schmidt, M. L., Lee, V. M., Trojanowski, J. Q., Jakes, R., and Goedert, M. (1997). Alpha-synuclein in Lewy bodies. *Nature* **388**, 839–840.

Swarup, G., and Nagabhushana, A. (2010). Optineurin, a multifunctional protein involved in glaucoma, amyotrophic lateral sclerosis and antiviral signalling. *J. Biosci.* **35**, 501–505.

Switzer, R. C., and Butt, M. T. (2011). Histological markers of neurotoxicity (nonfluorescent). In *Fundamental Neuropathology for Pathologists and Toxicologists* (B. Bolon, M. T. Butt, Eds.), pp. 181–190. Wiley, Hoboken.

Tan, C. C., Yu, J. T., Tan, M. S., Jiang, T., Zhu, X. C., and Tan, L. (2014). Autophagy in aging and neurodegenerative diseases: Implications for pathogenesis and therapy. *Neurobiol. Aging* **35**, 941–957.

Tanner, C. M., Kamel, F., Ross, G. W., Hoppin, J. A., Goldman, S. M., Korell, M., Marras, C., Bhudhikanok, G. S., Kasten, M., Chade, A. R., *et al.* (2011). Rotenone, paraquat, and Parkinson's disease. *Environ. Health Perspect.* **119**, 866–872.

Tapias, V., Cannon, J. R., and Greenamyre, J. T. (2010). Melatonin treatment potentiates neurodegeneration in a rat rotenone Parkinson's disease model. *J. Neurosci. Res*. **88**, 420–427.

Tapias, V., Cannon, J. R., and Greenamyre, J. T. (2014). Pomegranate juice exacerbates oxidative stress and nigrostriatal degeneration in Parkinson's disease. *Neurobiol. Aging* **35**, 1162–1176.

Visvikis, O., Ihuegbu, N., Labed, S. A., Luhachack, L. G., Alves, A. M., Wollenberg, A. C., Stuart, L. M., Stormo, G. D., and Irazoqui, J. E. (2014). Innate host defense requires TFEB-mediated transcription of cytoprotective and antimicrobial genes. *Immunity* **40**, 896–909.

Wild, P., Farhan, H., McEwan, D. G., Wagner, S., Rogov, V. V., Brady, N. R., Richter, B., Korac, J., Waidmann, O., Choudhary, C., *et al*. (2011). Phosphorylation of the autophagy receptor optineurin restricts Salmonella growth. *Science* **333**, 228–233.

Wong, Y. C., and Holzbaur, E. L. (2014). Optineurin is an autophagy receptor for damaged mitochondria in parkin-mediated mitophagy that is disrupted by an ALS-linked mutation. *Proc. Natl. Acad. Sci. U. S. A*. **111**, E4439–E4448.

Ying, H., and Yue, B. Y. (2012). Cellular and molecular biology of optineurin. *Int. Rev. Cell Mol. Biol*. **294**, 223–258.

Zharikov, A. D., Cannon, J. R., Tapias, V., Bai, Q., Horowitz, M. P., Shah, V., El Ayadi, A., Hastings, T. G., Greenamyre, J. T., and Burton, E. A. (2015). shRNA targeting alpha-synuclein prevents neurodegeneration in a Parkinson's disease model. *J. Clin. Invest*. **125**, 2721–2735.

Zhu, J. H., Guo, F., Shelburne, J., Watkins, S., and Chu, C. T. (2003). Localization of phosphorylated ERK/MAP kinases to mitochondria and autophagosomes in Lewy body diseases. *Brain Pathol*. **13**, 473–481.